An out-of-equilibrium non-Markovian Quantum Heat Engine

Marco Pezzutto[1,2], Mauro Paternostro[3], and Yasser Omar[1,2]
[1] *Instituto de Telecomunicações, Physics of Information and Quantum Technologies Group, Lisbon, Portugal*
[2] *Instituto Superior Técnico, Universidade de Lisboa, Portugal*
[3] *Centre for Theoretical Atomic, Molecular and Optical Physics, School of Mathematics and Physics, Queen's University Belfast BT7 1NN, United Kingdom*

We study the performance of a quantum Otto cycle using a harmonic work medium and undergoing collisional dynamics with finite-size reservoirs. We span the dynamical regimes of the work strokes from strongly non-adiabatic to quasi-static conditions, and address the effects that non-Markovianity of the open-system dynamics of the work medium can have on the efficiency of the thermal machine. While such efficiency never surpasses the classical upper bound valid for finite-time stochastic engines, the behaviour of the engine shows clear-cut effects induced by both the finiteness of the evolution time, and the memory-bearing character of the system-environment evolution.

I. INTRODUCTION

The study of work- and heat-exchanges at the quantum scale [1–3] is paving the way to the understanding of how quantum fluctuations influence the energetics of non-equilibrium quantum processes. In turn, such fundamental progress is expected to have significant repercussions on the design and functioning of quantum heat machines [4–9].

Such devices thus play the role of workhorses for the explorations of the potential advantages stemming from the exploitation of quantum resources for thermodynamic applications at the nano-scale [10, 11]. Theoretical models of microscopic heat engines based on the use of working fluid comprising two-level systems [12] or quantum harmonic oscillators [13] have been introduced. Such designs appear increasingly close to grasp in light of the recent progresses in the experimental management of (so far classical) thermal engines using individual particles [14, 15] or mechanical systems [16–18].

Is it possible to pinpoint genuine signatures of quantum behaviour that influence the thermodynamics of a system in ways that could never be produced by a classical mechanism [19]? How would quantum mechanics enhance the performance of a quantum thermal engine beyond anything achievable classically [20–23]? Do coherences in the energy eigenbasis [24–27] or non-thermal reservoirs [28, 29] represent exploitable (quantum) thermodynamic resources? In an attempt at providing answers to such burning questions, in this paper we study the finite-time thermodynamics of a heat engine operating an Otto cycle whose work fluid is a quantum harmonic oscillator. Hot and cold environments are modelled via a collections of spin-1/2 particles (Fig. 1). The work strokes of the cycle are implemented via parametric changes of the frequency of the harmonic oscillator, while heat exchanges result from *collisional* dynamics with the environments that may allow for memory effects [30]. The significant flexibility and richness of dynamical conditions of collisional models is perfectly suited to the exploration of non-Markovian dynamics in a wide range of conditions [31–38].

The scope of our study is twofold: on the one hand, we investigate work transformations of controlled yet variable duration, spanning the whole range from an infinitely slow (and thus adiabatic) transformations, to the opposite extreme of a sudden quench. On the other hand, by including intra-environment interactions, we allow for the emergence of memory effects and thus non-Markovianity in the dynamics of the engine. We investigate numerically the behaviour of the engine and its performance in the two cross-overs from adiabaticity to sudden quench, and from Markovianity to non-Markovianity. We aim at identifying the optimal trade-off between efficiency and speed, and the role and impact of memory effects on the engine performance.

Among the results reported in this paper is the demonstration that the efficiency of the device always decreases as we approach the sudden-quench regime, and the quantification of an optimal time at which the power output is maximum. Intra-environment interactions, in turn, seem to have no effect on the long-time engine performance. However, they affect the transient of the evolution of the engine by seemingly lowering the efficiency of the heat-transfer process – at least in the case when the both the engine and the environment particles are initialized in a thermal state. In no case we observe a performance exceeding the classical bounds, which is in agreement with the result reported in [19]. We do observe however a strong connection between non-Markovianity and the coherences in the initial engine state.

The remainder of the article is structured as follows. Sec. II introduces our model for heat engine, describing how the work and heat transformations are realized. Sec. III presents the results of our quantitative analysis, while in Sec. IV we draw our conclusions. Finally, Appendix A reviews key concepts of quantum non-Markovianity and its characterization used in our quantitative analysis.

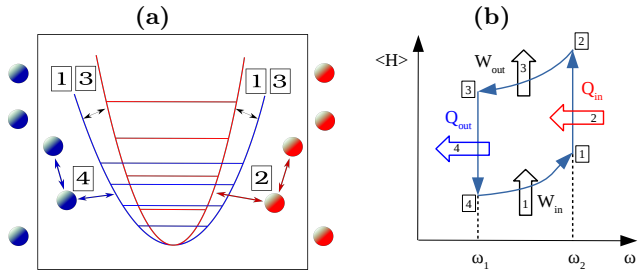

FIG. 1. **(a)** We study an engine performing an Otto cycle with a quantum harmonic oscillator as the working fluid, which in turn interacts with two environments composed of spin-1/2 particles. Work is done on/by the oscillator by changing the frequency of its potential, while in isolation from the environments (cf. Sec. II B). Heat is exchanged with the latter through collisions with the spin-1/2 particles (cf. Sec. II C). Additional intra-environment interactions allow the environments to keep memory of past interactions with the engine. **(b)** As its classical version, the cycle is composed by four strokes: two isentropic (strokes 1 and 3), where work is performed on or by the engine, and two (strokes 2 and 4), during which heat is exchanged with the reservoirs. In our model, the control parameter is the oscillator frequency ω, whose changes play the role of an effective modification in volume in the classical version of the engine. Therefore, strokes 2 and 4 are analogous to isocoric transformations. On the vertical axis, we report the average internal energy of the oscillator $\langle \hat{H} \rangle$, which quantifies the energy exchanges resulting from the four strokes.

II. THE ENGINE MODEL

We study a model of heat engine operating according to an Otto cycle, whose working fluid is a quantum harmonic oscillator governed by the Hamiltonian

$$H_{\rm s}(t) = \frac{p^2}{2m} + \frac{m\omega^2(t)x^2}{2}. \tag{1}$$

The subscript "s" stands for "system" as we may regard the engine as our main system of interest. The Otto cycle consists of two work strokes and two heat strokes. The work strokes are implemented by changing the frequency ω of the harmonic potential. The hot and cold environments are modelled as a collection of spin-1/2 particles with Hamiltonian

$$H_{\rm e}^{(n)} = \frac{1}{2}\hbar\omega_{\rm e}\sigma^{\rm z}_{{\rm e},n}, \qquad \omega_{\rm e} > 0, \qquad {\rm e} = {\rm c}, {\rm h}$$

for the n-th particle. The subscripts "h,c" stands for either a hot- or a cold-reservoir particle. The engine interacts with them through a collisional model, similar to the one employed in Ref. [35]. The details of these dynamical processes, pictured in Fig. 1, are outlined in following Subsections.

A. Details of the cycle operation and thermodynamics of the process

We are now going to outline the protocol through which the Otto cycle is implemented, and its thermodynamics. Let us define the thermodynamic quantities that will be central to our analysis.

We start with the *internal energy of the engine*, which is defined as

$$E := {\rm Tr}[\rho_{\rm s} H_{\rm s}]. \tag{2}$$

The second quantity of relevance is the *work* done on/by the engine during a work-producing stroke. As, in an Otto cycle, no heat is exchanged in one of such strokes, the difference between the values of the internal energy of the engine at the initial and final points of the stroke quantifies the exchanged work. We thus have

$$W := E_{\rm in}^{(k)} - E_{\rm fin}^{(k)}, \tag{3}$$

where $k = 1, 3$ identifies the work-producing strokes. In what follows, we use the usual convention that $W > 0$ when work is *performed* by the engine. This is also in agreement with a definition of the average exchanged work based on the so-called two-projective-measurement approach [39].

Similarly to the above considerations, no work is exchanged during a heat-exchanging stroke, so that the difference between the values of the internal energy of the engine at the initial and final points of the stroke provides an estimate of the exchanged *heat* Q. Therefore

$$Q := E_{\rm fin}^{(k)} - E_{\rm in}^{(k)}, \tag{4}$$

where $Q > 0$ if it is *absorbed* by the work medium, and $k = 2, 4$ is the label for the heat-producing strokes. An engine-environment interaction that conserves the total energy [such as the one illustrated in Sec. II C], is a physically sound description of a heat transfer process, as it is well suited to describe the heat exchange as a flow of energy from one system (engine or environment) to the other. Moreover, it is consistent with a more general definition of the exchanged heat as the *difference of the environment internal energy*.

The environmental particles are assumed to be all prepared in a single-particle thermal state,

$$\rho_{\rm e}^{(n)} = \frac{e^{-\beta_{\rm e} H_{\rm e}^{(n)}}}{{\rm Tr}\left[e^{-\beta_{\rm e} H_{\rm e}^{(n)}}\right]}$$

with $\beta_{\rm e} = 1/(\kappa T_{\rm e})$ the inverse temperature of the ${\rm e} = {\rm c}, {\rm h}$ environment. We have also assumed the hierarchy of temperatures $T_{\rm c} < T_{\rm h}$. The work fluid is assumed to be initialized in a thermal state at initial temperature $T_{\rm s}$ such that $T_{\rm c} < T_{\rm s} < T_{\rm h}$.

With reference to Fig. 1, our Otto cycle is implemented with the following steps:

Stroke 1–Compression: let the initial engine internal energy be E_0. The oscillator frequency is changed from ω_c to ω_h in isolation from any environment. The final energy is E_1 and the work *done on* the engine is $W_{in} = E_0 - E_1 < 0$.

Stroke 2a–Contact with hot environment: the engine interacts with a hot-environment particle and the final internal energy is E_2. The engine absorbs the heat $Q_{in} = E_2 - E_1 > 0$.

Stroke 2b–Intra-environment interaction: the internal interaction between the environmental particles may propagate some memory of the engine state and feed it back at a later stage. This step has no direct effect on the thermodynamics of the engine.

Stroke 3–Expansion: the oscillator's frequency is changed from ω_h back to ω_c in isolation from any environment. The final energy is E_3 and the work *performed by* the engine is $W_{out} = E_3 - E_2 > 0$.

Stroke 4a–Contact with cold environment: the engine interacts with a cold-environment particle and the final internal energy is E_4. The engine has transferred an amount of heat $Q_{out} = E_4 - E_3 < 0$ to the environment.

Stroke 4b–Intra-environment interaction: similar to stroke 2b.

The final state of the engine becomes the initial state of a new cycle and the steps are iterated, involving new environmental particles. The dynamics thus proceeds through discrete time steps, each of them being a full iteration of the Otto cycle. At the end of each cycle, we compute the *power* output of a cycle, and its *efficiency*. By denoting with $\mathcal{T}$ the total duration of one cycle, the power output is $P := (W_{in}+W_{out})/\mathcal{T}$, while the efficiency reads $\eta := (W_{in} + W_{out})/Q_{in}$.

Let us recall the usual expression for the internal energy of a quantum harmonic oscillator $E = \hbar\omega(1/2 + \langle n\rangle)$ with n the number operator. Let us define as $n_i = \langle n\rangle_i$ $(i = 0, \dots, 4)$ the average occupation number at the beginning $(i = 0)$ and after step $i \geq 1$ of the protocol, such that $E_i = \hbar\omega_e(1/2 + n_i)$, with $\omega_e = \omega_c$ at the beginning and after strokes 3 and 4, and $\omega_e = \omega_h$ after strokes 1 and 2. We finally assume $n_4 = n_0$ if the engine performs a stationary cycle. Using Eqs. (2)-(4) we have

$$\eta = \frac{E_2 - E_3 + E_0 - E_1}{E_2 - E_1} = 1 - \frac{\omega_c(n_3 - n_0)}{\omega_h(n_2 - n_1)}.$$

If the work transformations are performed adiabatically, the populations remain unchanged, thus $n_1 = n_0$ and $n_2 = n_3$, leading to the remarkably simple theoretical efficiency

$$\eta_{th} = 1 - \frac{\omega_c}{\omega_h}, \tag{5}$$

irrespectively of the details of the heat exchanges.

B. Work transformations

The work strokes are implemented through a unitary transformation on the engine alone, isolated from the cold or hot environment. A theoretical description of such processes was developed in Ref. [40] and further extended in Ref. [39]. In the following, we summarise the key steps of this treatment, which represent the basis for our implementation of the work strokes.

We wish to find a wave-function $\psi(x, t)$ satisfying the Schrödinger equation

$$i\hbar\partial_t\psi(x, t) = H_s(t)\psi(x, t) \tag{6}$$

within the time interval $[0, \tau]$, with $\omega(0) = \omega_1$ and $\omega(\tau) = \omega_2$. In the following, ω_1 and ω_2 will be either ω_c or ω_h depending on which work transformation is being performed. The Hamiltonian in Eq. (1) can be written, at any *fixed* time t, in the second quantization formalism as

$$H_s(t) = \hbar\omega(t)\big(1/2 + a^\dagger(t)a(t)\big), \tag{7}$$

where the operators

$$a(t) = \sqrt{\frac{m\omega(t)}{2\hbar}}x + i\sqrt{\frac{1}{2m\hbar\omega(t)}}p \tag{8}$$

and $a^\dagger(t) = [a(t)]^\dagger$ depend explicitly on time. From Eq. (7), we obtain the instantaneous eigenvalues $E_n^t = \hbar\omega(t)(1/2 + n(t))$ and the wave-function $\phi_n^t(x)$ of its eigenvectors, which are just a slight generalization of the solutions for the time-independent quantum harmonic oscillator. Explicitly

$$\phi_n^t(x) = \sqrt[4]{\frac{m\omega(t)}{\pi\hbar}}\frac{1}{\sqrt{2^n n!}}e^{-\frac{m\omega(t)}{2\hbar}x^2}H_n\left(x\sqrt{\frac{m\omega(t)}{\hbar}}\right), \tag{9}$$

where $H_n(z)$ is the n-th Hermite polynomial of argument z. The superscript t aims at reminding that t here plays just the role of a label.

It can be seen by direct inspection that Eq. (6) admits solutions satisfying the Gaussian ansatz

$$\psi(x, t) = \exp\left[i\big(A(t)x^2 + 2B(t)x + C(t)\big)/2\hbar\right]. \tag{10}$$

By inserting this formula into Eq. (6), we obtain a system of three differential equation for the coefficients A, B, C reading

$$\frac{dA}{dt} = -\frac{A^2}{m} - m\omega^2(t) \tag{11}$$

$$\frac{dB}{dt} = -\frac{A}{m}B \tag{12}$$

$$\frac{dC}{dt} = i\hbar\frac{A}{m} - \frac{1}{m}B^2. \tag{13}$$

Eq. (11) can be mapped into the equation of motion of a classical time-dependent oscillator with amplitude $X(t)$,

through the substitution $A = m\dot{X}/X$. Explicitly

$$\frac{d^2X}{dt^2} + \omega^2(t)X = 0. \tag{14}$$

Once a parametrization is chosen for the transformation $\omega(t)$, solving such equation gives $A(t)$, from which also $B(t)$ and $C(t)$ can be found by integrating Eqs. (12) and (13). In [39] it is shown that by choosing the parametrization

$$\omega^2(t) = \omega_2^2 + t(\omega_1^2 - \omega_2^2)/\tau,$$

an analytic solution to such problem can be found. We refer to the mentioned reference for the full expression. Another key result, obtained in Ref. [40], is the expression of the propagator

$$U(x,\tau|x_0,0) = \sqrt{\frac{m}{2\pi i\hbar X(\tau)}}\, e^{\frac{im}{2\hbar X(\tau)}(\dot{X}(\tau)x^2 - 2xx_0 + Y(\tau)x_0^2)}, \tag{15}$$

where now $X(t)$ and $Y(t)$ are two specific solutions of Eq. (14) satisfying the boundary conditions

$$X(0) = 0, \qquad \dot{X}(0) = 1,$$
$$Y(0) = 1, \qquad \dot{Y}(0) = 0.$$

Having the explicit form of the propagator $U(x,\tau|x_0,0)$, we now have all the tools to describe the effect of the work transformation $\omega_1 \to \omega_2$ (for arbitrary values of $\omega_{1,2}$) on the engine density operator $\rho(x,y;t)$, considered here as dependent on position. We have

$$\rho(x_0,y_0;0) \mapsto$$
$$\rho(x,y;\tau) = \int U(x,\tau|x_0,0)\rho(x_0,y_0;0)U^\dagger(y,\tau|y_0,0)\mathrm{d}x_0\mathrm{d}y_0 \tag{16}$$

One further step is required, with the aim of making the above transformation amenable to numerical treatment: the expansion of both the density matrix ρ and the operator U on the basis given by the eigenfunctions in Eq. (9). Let us define

$$\rho_{mn}(t) := \langle\phi_m^t|\rho(t)|\phi_n^t\rangle, \tag{17}$$
$$U_{mn} := \langle\phi_m^\tau|U(\tau,0)|\phi_n^0\rangle, \tag{18}$$

where we omitted the position dependencies since they are integrated over in the scalar products. It should be stressed that the U_{mn} elements are computed by taking scalar products with two *different* sets of eigenfunctions, the effect of $U(\tau,0)$ being precisely that of implementing the transformation from one Hamiltonian to another. Eq. (16) then becomes

$$\rho_{mn}(0) \mapsto \rho_{kl}(\tau) = \sum_{mn} U_{km}\rho_{mn}(0)U_{nl}^\dagger.$$

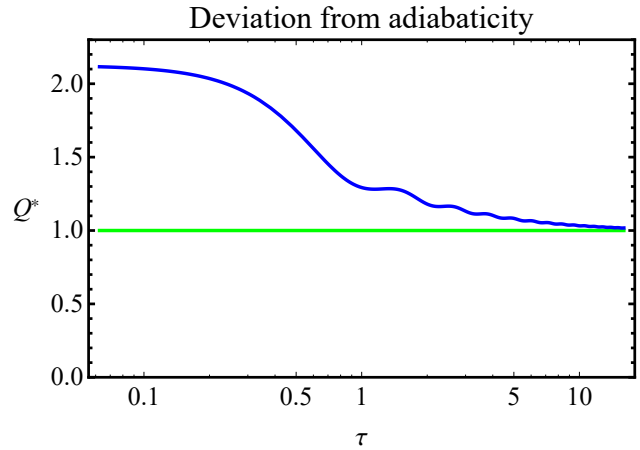

FIG. 2. Deviation from the adiabatic regime, as captured by the Q^* factor as a function of the work stroke duration τ, for $\omega_1 = 1$ and $\omega_2 = 4$. The green (lighter) line represents the limit $Q^* = 1$ for $\tau \to \infty$.

In Ref. [40] an expression for the generating function of transition probabilities from the initial to the final eigenstates $P_{m,n}^\tau = |\langle\phi_m^\tau|U(\tau,0)|\phi_n^0\rangle|^2$ is provided:

$$P(u,v) = \sum_{m,n} u^m v^n P_{m,n}^\tau$$
$$= \sqrt{\frac{2}{Q^*(1-u^2)(1-v^2) + (1+u^2)(1+v^2) - 4uv}},$$

Remarkably, the above expression depends on the details of the parametrization $\omega(t)$ only through the factor Q^*, whose expression for the most general transformation is provided in [39]:

$$Q^* = \frac{\omega_1^2\left(\omega_2^2 X(\tau)^2 + \dot{X}(\tau)^2\right) + \left(\omega_2^2 Y(\tau)^2 + \dot{Y}(\tau)^2\right)}{2\omega_1\omega_2} \tag{19}$$

The factor tends to the limiting value $Q^* \to 1$ for $\tau \to \infty$, and becomes increasingly greater than 1 as τ becomes smaller, as exemplified in Fig. 2.

The following special cases are of particular interest:

- *No transformation is performed*, $\omega_2 = \omega_1$. It can be shown that the propagator (15) becomes the identity operator embodied by $U(x,\tau|x_0,0) = \delta(x-x_0)$. The matrix elements (18) are $U_{mn} = \delta_{mn}$, since the initial and final eigenbasis coincide.

- *Sudden quench*, $\tau \to 0$. Also in this case $U(x,\tau|x_0,0) \to \delta(x-x_0)$, because the transformation is so quick that the density operator is left unchanged. Its matrix elements ρ_{mn}, however, undergo a unitary change of basis through the matrix $U_{mn} = \langle\phi_m^{(2)}|\phi_n^{(1)}\rangle$, where the superscripts refer to the frequencies ω_1, ω_2.

- *Adiabatic transformation*, $\tau \to \infty$. The initial eigenstates are mapped one-to-one to the final ones,

infinitely slowly. The propagator can be expressed as $U(\tau,0)=\sum_n |\phi_n^\tau\rangle\langle\phi_n^0|$, which gives $U_{mn}=\delta_{mn}$.

From now on, we will denote the duration τ of the work transformations by $\tau_{\rm w}$.

C. Heat exchanges: collisional model

Let us now introduce the model for the environments and for how they interact, both with the engine and within themselves. The interactions are implemented through a *collisional model.* When the engine interacts, say, with the cold environment, it undergoes an interaction with one, and only one, environment particle at a time, through a *unitary* operator acting non-trivially only on the Hilbert spaces of the engine and said particle. This is what we refer to as a *collision*, meaning a "point-like" interaction between the engine and one element of the environment. With the thermodynamic limit in sight, it is assumed that the engine never interacts twice with the same environment particle: at each collision, the engine interacts with a new, "fresh" particle.

The unitary $V_{\rm se}$ through which the interaction happens is generated by a resonant excitation conserving Hamiltonian

$$H_{\rm se}=J\big(a\sigma_{\rm e}^{+}+a^\dagger\sigma_{\rm e}^{-}\big), \tag{20}$$

$$V_{\rm se}=\exp\Big[-\frac{i}{\hbar}H_{\rm se}\tau_{\rm se}\Big],\qquad {\rm e}={\rm c},{\rm h} \tag{21}$$

where the main coupling constant J and the interaction time $\tau_{\rm se}$ rule the interaction strength, and are assumed to be the same for both environments. As mentioned in Sec. II A, at the moment of interaction the engine frequency matches exactly that of the environment particle it is interacting with. In the most basic, completely memoryless implementation of such a model, only one particle for each environment actually stored at any time. Indicating by $\mathcal{H}_{\rm s}$, $\mathcal{H}_{\rm c}$ and $\mathcal{H}_{\rm h}$ Hilbert spaces of the engine, of a cold and a hot particle respectively, the minimal total Hilbert space is

$$\mathcal{H}=\mathcal{H}_{\rm c}\otimes\mathcal{H}_{\rm s}\otimes\mathcal{H}_{\rm h}.$$

With reference to Fig. 1 **(a)**, suppose the engine is in the state $\rho_{\rm s}$ at the beginning of iteration n of the thermodynamic cycle, and interacts with the n-th cold particle initially in the state $\rho_{\rm c}^{(n)}$,

$$\rho_{\rm c}^{(n)}\otimes\rho_{\rm s}\otimes\rho_{\rm h}^{(n)}\to$$
$$\tilde\rho_{\rm csh}=(V_{\rm sc}\otimes\mathbb{I}_{\rm h})\big(\rho_{\rm c}^{(n)}\otimes\rho_{\rm s}\otimes\rho_{\rm h}^{(n)}\big)(V_{\rm sc}^\dagger\otimes\mathbb{I}_{\rm h}),$$

and a hot particle $\rho_{\rm h}^{(n)}$, while present, is left unaffected [41]. After interaction, we take the local marginals of both parties $\tilde\rho_{\rm s}={\rm Tr}_{\rm c,h}[\tilde\rho_{\rm csh}]$ and $\tilde\rho_{\rm c}^{(n)}={\rm Tr}_{\rm s,h}[\tilde\rho_{\rm csh}]$ and possibly use them to compute the various thermodynamic quantities as explained in Sec. II A. The particle $\rho_{\rm c}^{(n)}$ is then discarded, in practice traced away from the global density matrix, and a new one $\rho_{\rm c}^{(n+1)}$ is included in the model in its place, such the global state ready for the next step is

$$\rho_{\rm c}^{(n+1)}\otimes\tilde\rho_{\rm s}\otimes\rho_{\rm h}^{(n)}$$

We now take a step further and introduce intra-environment collisions, thus allowing the environments to carry over memory of past interactions with the engine, opening the possibility for the engine dynamics to be non-Markovian. We wish therefore to consider two particles for each environment at any given time. In order to do so, we need to extend the Hilbert space we work with to

$$\mathcal{H}=\mathcal{H}_{{\rm c},b}\otimes\mathcal{H}_{{\rm c},a}\otimes\mathcal{H}_{\rm s}\otimes\mathcal{H}_{{\rm h},a}\otimes\mathcal{H}_{{\rm h},b},$$

where the additional subscript "a" indicates now the first (hot or cold) environment particle interacting with the engine and "b" indicates the second, that is particles n and $n+1$ in our example. Before is it traced away, the environment particle n undergoes a further collision with the particle $n+1$, through a Heisenberg interaction Hamiltonian:

$$H_{\rm ee}=J_{\rm ee}\big(\sigma_n^{\rm x}\sigma_{n+1}^{\rm x}+\sigma_n^{\rm y}\sigma_{n+1}^{\rm y}+\sigma_n^{\rm z}\sigma_{n+1}^{\rm z}\big), \tag{22}$$

$$V_{\rm ee}=\exp\Big[-\frac{i}{\hbar}H_{\rm ee}\tau_{\rm ee}\Big],\qquad {\rm ee}={\rm cc},{\rm hh} \tag{23}$$

with coupling constant $J_{\rm cc}(J_{\rm hh})$ and interaction time $\tau_{\rm cc}(\tau_{\rm hh})$ for the cold (hot) environment. As explained in [42], [32] and [35], the interaction acts effectively as a *partial swap*, exchanging the states of the two particles with probability $\sin^2(2J_{\rm ee}\tau_{\rm ee})$. In particular, a perfect swap is achieved for $J_{\rm ee}\tau_{\rm ee}=\pi/4$.

Continuing in our example, after the subsequent application of $V_{\rm sc}$ and $V_{\rm cc}$, the engine and particle $n+1$ will be in general in a *correlated state*, $\tilde\rho_{\rm sc}^{(n+1)}$ *even if they haven't interacted directly yet.* After tracing away the cold particle n, "shifting" particle $n+1$ from position c,b to c,a in our Hilbert space, and including a new particle $n+2$ in position (c,b), the global state is

$$\rho_{\rm c}^{(n+2)}\otimes\tilde\rho_{\rm sc}^{(n+1)}\otimes\rho_{\rm h}^{(n)}\otimes\rho_{\rm h}^{(n+1)}.$$

This completes the description of one full heat stroke. The state is now ready for the next stroke, which will be a work one. The interactions between the engine and the hot environment, and within the hot environment, would occur in exactly the same way. Therefore, at the end of a full cycle, composed of all the steps of Sec. II A, the global state looks like

$$\rho_{\rm c}^{(n+2)}\otimes\tilde\rho_{\rm sch}^{(n+1)}\otimes\rho_{\rm h}^{(n+2)},$$

with the engine correlated to the hot and cold particles $(n+1)$. More details on this model of system-environment interaction can be found in [35].

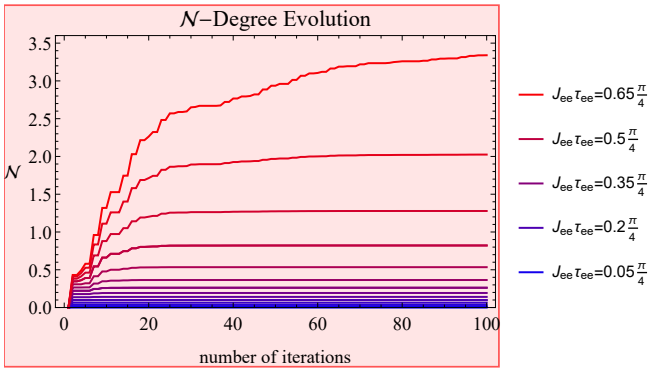

FIG. 3. Signatures of non-Markovianity: time evolution of the degree of non-Markovianity $\mathcal{N}$, with intra-environment interaction $J_{\rm ee}\tau_{\rm ee}$ increasing from blue to red (bottom to top). Nearly adiabatic work strokes ($J\tau_{\rm w} = 32$) and pure initial states $|\psi^{\pm}_{\rm test}\rangle$. **Inset:** final $\mathcal{N}$ against the intra-environment interaction $J_{\rm ee}\tau_{\rm ee}$. The dashed line is a guide for the eye.

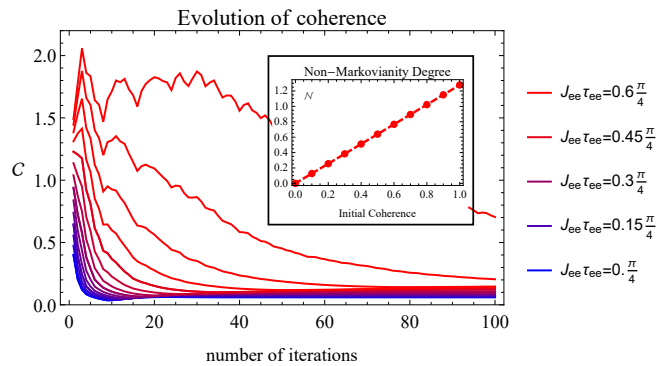

FIG. 4. Time evolution of the coherence $\mathcal{C}$ in the engine density matrix, with intra-environment interaction $J_{\rm ee}\tau_{\rm ee}$ increasing from blue to red (bottom to top). Pure initial states $|\psi^{\pm}_{\rm test}\rangle$. The work strokes are nearly adiabatic, $J\tau_{\rm w} = 32$. **Inset:** degree of non-Markovianity $\mathcal{N}$ against initial coherence in the pure initial states $|\psi^{\pm}_{\alpha}\rangle$, with α on the x axis. The dashed line is a guide for the eye.

Finally, the total cycle duration is $\mathcal{T} = 2(\tau_{\rm w} + \tau_{\rm se})$, taking into account only the steps in which the engine is directly involved and assuming the intra-environment interactions to occur at the same time as the work strokes.

III. RESULTS

We present here the results on the engine performance and the possible influence of non-Markovianity on its operations. First, we present evidence of non-Markovianity in the engine dynamics and its dependence on intra-environment interactions. We then investigate the crossover from adiabatic to sudden quench work strokes in the purely Markovian regime. Finally we show how the non-Markovianity affects the engine performance.

Few words on the choice of parameters. We work in units where $\hbar = 1, \kappa = 1$, and also choose $J = J_{\rm cc} = J_{\rm hh} = 1$ without loss of generality. The temperatures of the environments are $T_{\rm c} = 0.1$ and $T_{\rm h} = 10$, giving a Carnot efficiency of 0.99 and a Curzon-Ahlborn efficiency of 0.9 as theoretical upper bounds. The engine is initialized in a thermal state at $T_{\rm s} = 0.5$ unless otherwise stated. While the initial temperature is not very crucial for the thermodynamics, the fact of the initial state being diagonal in the energy eigenbasis does impact the behaviour of the engine.

We chose an interaction between the engine and the environments of moderate strength $J\tau_{\rm se} = 0.3$, in order for it to be quite weak, but not so weak that the heat exchanged per cycle becomes too small, compared to the exchanged work. The chosen environment frequencies are $\omega_{\rm c} = 1$ and $\omega_{\rm h} = 4$, close enough to each other that the work exchanged is not too big, compared to the exchanged heat, and such that the adiabatic regime ($\tau_{\rm w} \to +\infty$) is approximated well at $\tau_{\rm w} = 16$ and very well at $\tau_{\rm w} = 32$. The gap between $\omega_{\rm h}$ and $\omega_{\rm c}$ is nonetheless big enough that, in the sudden quench regime, the Q^* factor is appreciably different from 1, in fact surpassing 2 as can be seen in Fig. 2. The theoretical efficiency in the adiabatic case is $\eta_{\rm th} = 0.75$.

The density matrices of the environment particles are represented in the eigenbasis $\{\,|0\rangle\,, |1\rangle\,\}$ of the Hamiltonian $\hbar\omega_{\rm e}\sigma^{\rm z}_{\rm e}/2$.

As the initial temperature $T_{\rm s}$ is low, the initial populations decay quite fast, being negligible (below machine precision) above level $n = 20$. Therefore, in most simulations we could safely truncate the Fock space at $n = 30$, checking that the matrices representing the unitaries U, $V_{\rm se}$, and $V_{\rm ee}$ in the truncated space remain approximately unitary. We performed tests extending the Fock space up to $n = 50$ to confirm that the results were not appreciably different than those obtained truncating at $n = 30$. Since at any time we simulate two particles for each environment, the dimension of the total dimension of the density matrix is $2^4 \times 31 = 496$.

A. Non-Markovianity of the engine dynamics

As summarized in Appendix A, in order to quantify the degree of non-Markovianity $\mathcal{N}$ according to the BLP measure, one has to choose pairs of initial states, make them evolve in time according to the specific dynamics in object, and observe the behaviour of the trace distance. It is then required to maximise $\mathcal{N}$ over all possible choices of initial pairs. In our case, however, the state of the engine is represented by a 31×31 complex hermitian matrix and the maximization is an extremely demanding task. We chose therefore heuristically a couple of pure orthogonal states $|\psi^{\pm}_{\rm test}\rangle$, guided by analogy with the spin-1/2 particle case in which often the optimal

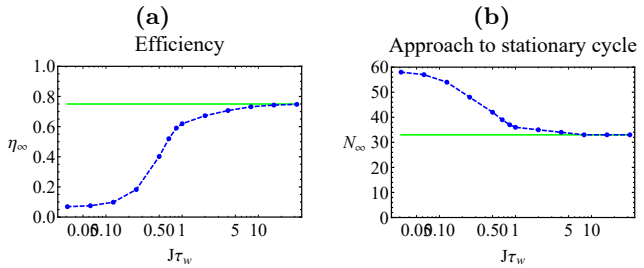

FIG. 5. **(a)** Stationary cycle efficiency η_∞ against the duration of the work stroke τ_w, for engine-environment coupling constant $J = 1$. The dashed line is a guide for the eye, the green (solid) line represents the theoretic adiabatic efficiency $\eta_\mathrm{th} = 1 - \omega_c/\omega_h$. **(b)** Number of iterations N_∞ required to reach the stationary cycle against the duration of the work stroke τ_w, for engine-environment coupling constant $J = 1$. The dashed line is a guide for the eye, the green (solid) line represents the limit $\tau_\mathrm{w} \to \infty$.

pair is $|\pm\rangle = (|0\rangle \pm |1\rangle)/\sqrt{2}$ [32, 35]. The choice was

$$\left|\psi^{\pm}_{\mathrm{test}}\right\rangle = \frac{|0\rangle \pm |10\rangle}{\sqrt{2}}, \tag{24}$$

as we found that pure states in the form $(|0\rangle \pm |n\rangle)/\sqrt{2}$, with a high degree of coherence in the energy eigenbasis, seem to be particularly favourable to boost the non-Markovianity measure. This particular choice $\left|\psi^{\pm}_{\mathrm{test}}\right\rangle$ turned out to be the one yielding the biggest $\mathcal{N}$. Even though we do not have evidence that this is the best pair of states maximising the non-Markovianity degree $\mathcal{N}$, we are confident that the results may still provide a valuable insight on the non-Markovian character of the dynamics.

Fig. 3 presents the behaviour of the non-Markovianity degree $\mathcal{N}$ in its dependence on the intra-environment interaction strength and in its time evolution, in the case of adiabatic work strokes. The non-Markovian behaviour is intrinsically a property of the dynamics during the transient to stationary state. Fig. 4 shows the dynamics of the total internal coherence of the engine, quantified by

$$\mathcal{C} := \sum_{i \neq j} |\rho_{ij}|.$$

The coherence in the stationary state settles to a quite small value, irrespective of the initial state. Furthermore, the more the dynamics is non-Markovian, the longer the coherences survive. This is most likely a direct consequence of the fact that the interaction with non-Markovian environments slows down the approach to the stationary state (see also Fig. 7). The inset of Fig. 4 shows the relation between non-Markovianity and the initial coherence present in the engine, when initialized in the state $|\psi^{\pm}_{\alpha}\rangle = (|0\rangle \pm \alpha\,|10\rangle)/N_\alpha$, normalized by N_α, with $\alpha = m \times 0.1$, $m = 0, 1, \ldots, 10$. The connection between the presence of coherence in the initial states and their effectiveness in the detection of non-Markovianity is evident.

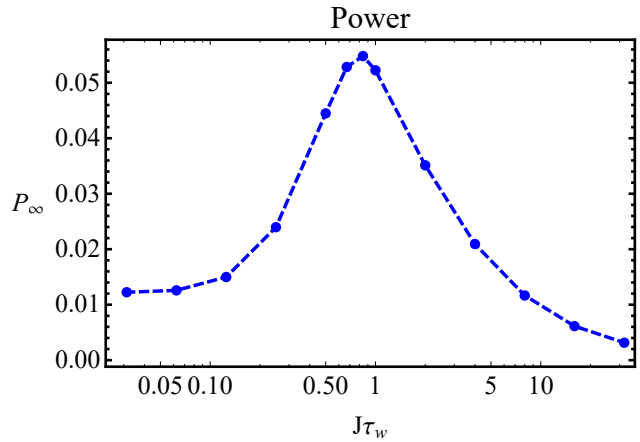

FIG. 6. Power output against the duration of the work stroke τ_w, for engine-environment coupling constant $J = 1$. The dashed line is a guide for the eye. The power vanishes for $\tau_\mathrm{w} \to \infty$, as the efficiency approaches the limit η_th while the cycle duration grows as $\sim 2\tau_\mathrm{w}$. In the sudden quench limit, instead, it approaches a finite value, being η non-zero for $\tau_\mathrm{w} \to 0$ while the cycle duration is $\sim 2\tau_\mathrm{se}$.

B. Engine performance

Fig. 5 and 6 summarize the behaviour of the engine in the Markovian regime, with no intra-environment interactions, focusing on the crossover from adiabatic to sudden quench work strokes. We can see that the stationary cycle efficiency η_∞ reaches the expected limit η_th in the adiabatic case, and decreases as we depart from adiabaticity. The duration of the work strokes τ_w also affects the number of iterations N_∞ it takes for the engine to reach the stationary regime, which grows as we approach the sudden quench regime. This further indicates a drop of the engine performance as we move away from adiabaticity. The power output per single iteration P_∞, however, has a maximum around $\tau_\mathrm{w} = 1$, since at that point the efficiency deviates only slightly from η_th.

Fig. 7 and 8 present the behaviour of the performance in the most general case of the engine operating with non-adiabatic work strokes and non-Markovian environments. Non-Markovianity seem to always affect negatively the performance, but it does so more pronouncedly as we deviate from the adiabatic regime. In particular, the efficiency in the adiabatic case is mostly independent of the non-Markovian character of the dynamics, approaching in fact η_th, while for smaller durations of the work strokes it drops more pronouncedly as the intra-environment interactions become stronger. The power output, therefore, decreases accordingly.

IV. CONCLUSIONS AND OUTLOOK

In this work we studied the out-of-equilibrium thermodynamics and performance of a quantum Otto cycle

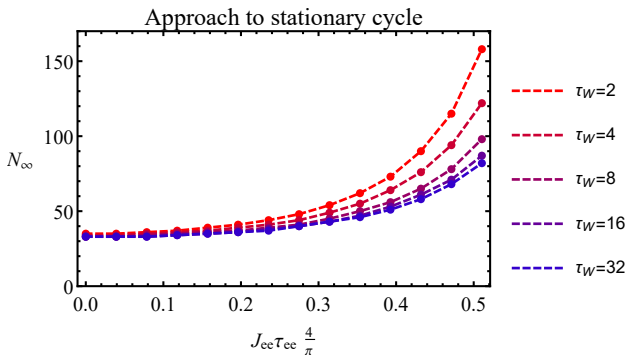

FIG. 7. Number of iterations N_∞ to the stationary cycle, against the intra-environment interaction $J_{ee}\tau_{ee}$. The dashed lines are guides for the eye. The duration τ_w of the work strokes increases from the red to the blue curve (top to bottom).

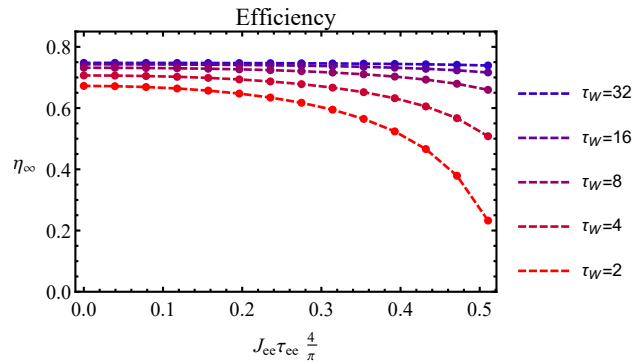

FIG. 8. Stationary cycle efficiency η_∞ against the intra-environment interaction $J_{ee}\tau_{ee}$. The dashed lines are guides for the eye. The duration τ_w of the work strokes decreases from the blue to the red curve (top to bottom).

employing a harmonic oscillator as working fluid, in interaction with a finite-size environment through a collisional dynamics that may allow for memory effects, and thus for the emergence of non-Markovianity. We explored the crossover from adiabatic to sudden quench work strokes and found that, while departing from the adiabatic regime induces a drop in the efficiency, it is possible to find an optimal duration of the work strokes such that the power output is maximised. We do not observe better than classical performance, at least in the case when the both the engine and the environment particles are initialized in thermal states, which is consistent with the what reported in [19] on the thermodynamics of heat machines with quantized energy levels. Non-Markovianity signatures are observed in the engine dynamics, and even though such memory effects do not impact the stationary engine performance, they do affect the approach to the asymptotic cycle, slowing it down. Non-Markovianity is however found to be closely connected with the presence of initial coherences in the energy eigenbasis of the engine.

ACKNOWLEDGMENTS

M Pezzutto thanks the Centre for Theoretical Atomic, Molecular, and Optical Physics, School of Mathematics and Physics, Queen's University Belfast for hospitality during the development of this work. M Pezzutto and Y Omar thank the support from Fundação para a Ciência e a Tecnologia (Portugal) through programmes PTDC/POPH/POCH and projects UID/EEA/50008/2013, IT/QuNet, ProQuNet, partially funded by EU FEDER, from the QuantERA project TheBlinQC, and from the JTF project NQuN (ID 60478). Furthermore, M Pezzutto acknowledges the support from the DP-PMI and FCT (Portugal) through scholarship SFRH/BD/52240/2013. M Paternostro acknowledges support from the EU Collaborative project TEQ (grant agreement 766900), the DfE-SFI Investigator Programme (grant 15/IA/2864), the Royal Society Newton Mobility Grant NI160057, and COST Action CA15220. All authors gratefully acknowledge support from the COST Action MP1209.

Appendix A: Quantum non-Markovianity

Recently, the issue of non-Markovianity of quantum dynamics has received considerable attention aimed at characterizing the phenomenology of non-Markovian open-system dynamics through general tools of broad applicability. Such efforts are based on the formal assessment of the various facets with which non-Markovianity is manifested.

One of such approaches to the definition of Markovianity is based on the notion of *divisibility* [43]: a dynamical process is said to be Markovian if, for any two times $t \leq s$ there is a completely positive map $\Gamma(s,t)$ such that $\rho(s) = \Gamma(s,t)\rho(t)$, and such maps form a semigroup. The requirement of complete positivity links very tightly Markovianity with the behaviour of the dynamical maps on entangled states, in the sense that a Markovian process is always expected to degrade entanglement. In order to assess the (non-)Markovian character of the dynamics, one needs to perform a tomography of the process so as to reconstruct the map Γ.

Another widely employed approach, introduced in Refs. [44, 45], is based on the concept of information backflow. The starting point is the fact that any completely positive trace-preserving (CPTP) map is a *contraction* for the *trace distance* [46], defined as

$$D(\rho_1, \rho_2) := \tfrac{1}{2}\|\rho_1 - \rho_2\|\,,$$

where $\|A\| = \mathrm{Tr}\sqrt{A^\dagger A}$ is the trace-1 norm and $\rho_{1,2}$ are two density matrix of the system under scrutiny. The trace distance is a metric in the space of density matrices, closely related to their distinguishability: a value of

$D(\rho_1, \rho_2) = 1$ implies perfect distinguishability.

The contractive character of $D(\rho_1, \rho_2)$ under CPTP maps is the key idea for the quantification of non-Markovianity based on information backflow: Markovian maps can not increase the distinguishability of any two given states. If, however, one can find a pair of initial states and a time t for which contractivity is violated, resulting in

$$\sigma(t) = \frac{dD(\rho_1(t), \rho_2(t))}{dt} > 0, \tag{A1}$$

this is held as a signature of non-Markovianity in the dynamics. Such criterion can be used to build a quantitative measure $\mathcal{N}$ of non-Markovianity as

$$\mathcal{N} := \max_{\{\rho_1, \rho_2\}} \int_{\Sigma_+} \sigma(t) \mathrm{d}t, \tag{A2}$$

where Σ_+ is the time window where $\sigma(t) > 0$, and maximise on the choice of initial states. While finding the optimal pair of initial states is in general challenging, the task is often simplified owing to the result reported in Ref. [47], where it is proven that the states maximizing $\mathcal{N}$ must be orthogonal and belonging to the boundary of the state space.

[1] Talkner P, Lutz E and Hänggi P. Fluctuation theorems: Work is not an observable. *Phys. Rev. E* **75** 050102(R) (2007)

[2] Gallego R, Eisert J, and Wilming H. Thermodynamic work from operational principles *New J. Phys.* **18**, 103017 (2016)

[3] Goold J, Paternostro M, Modi K Non-equilibrium quantum Landauer principle *Phys. Rev. Lett.* **114** 060602 (2015)

[4] Quan H T, Liu Y, Sun C P and Nori F. Quantum thermodynamic cycles and quantum heat engines. *Phys. Rev. E* **76** 031105 (2007)

[5] Ghosh A, Niedenzu W, Mukherjee V and Kurizki G. Thermodynamic principles and implementations of quantum machines. arXiv:1803.10053 (2018)

[6] Seah S, Nimmrichter S, Roulet A, Scarani V. Quantum Rotor Engines. arXiv:1804.11023 (2018)

[7] Esposito M and Lindenberg K. Universality of Efficiency at Maximum Power. *Phys. Rev. Lett.* **102** 130602 (2009)

[8] Gelbwaser-Klimovsky D, Alicki R and Kurizki G. Minimal universal quantum heat machine *Phys. Rev. E* **87** 012140 (2013)

[9] Gardas B and Deffner S. Thermodynamic universality of quantum Carnot engines *Phys. Rev. E* **92** 042126 (2015)

[10] Scovil H Schulz-duBois E. Three-level masers as heat engines. *Phys. Rev. Lett.* **2** 262 (1959)

[11] Alicki R. The quantum open system as a model of the heat engine. *J. Phys. A* **12** 5 (1979)

[12] Linded N, Popescu S and Skryzypczyk P. How small can thermal machines be? The smallest possible refrigerator. *Phys. Rev. Lett. 105*, 130401 (2010)

[13] Kosloff R, Rezek Y. The Quantum Harmonic Otto Cycle. *Entropy* **19(4)** 136 (2017)

[14] Abah O, Rossnagel J, Jacob G, Deffner S, Schmidt-Kaler F, Singer K and Lutz E. Single ion heat engine with maximum efficiency at maximum power. *Phys. Rev. Lett.* **109** 203006 (2012)

[15] Roßnagel J, Dawkins S T, Tolazzi K N, Abah O, Lutz E, Schmidt-Kaler F, Singer K. A single-atom heat engine. *Science* **352** 6283 (2016)

[16] Zhang K, Bariani F and Meystre P. Quantum Optomechanical Heat Engine. *Phys. Rev. Lett.* **112** 150602 (2014)

[17] Zhang K, Bariani F and Meystre P. Theory of an optomechanical quantum heat engine. *Phys. Rev.A* **90** 023819 (2014)

[18] Dong Y, Zhang K, Bariani F and Meystre P. Work measurement in an optomechanical quantum heat engine. *Phys. Rev.A* **92** 033854 (2015)

[19] Gelbwaser-Klimovsky D, Bylinskii A, Gangloff D, Islam R, Aspuru-Guzik A and Vuletic V. Single-Atom Heat Machines Enabled by Energy Quantization. *Phys. Rev. Lett.* **120** 170601 (2018)

[20] Niedenzu W, Gebelwaser-Klimovsky D, Kofman A G and Kurizki G. On the operation of machines powered by quantum non-thermal baths *New J. Phys.* **18**, 083012 (2016)

[21] Campisi M, Pekola J and Fazio R. Nonequilibrium fluctuations in quantum heat engines: theory, example, and possible solid state experiments. *New J. Phys.* **17** 035012 (2015)

[22] Quantum heat engine operating between thermal and spin reservoirs. Wright J S S T, Gould T, Carvalho A R R, Bedkihal S and Vaccaro J A. *Phys. Rev.A* **97** 052104 (2018)

[23] Abah O and Lutz E. Effciency of heat engines coupled to nonequilibrium reservoirs. *Europhys. Lett.* **106** 20001 (2014)

[24] Scully M O, Zubairy M S, Agarwal G S and Walter H. Extracting work from a single heat bath via vanishing quantum coherence *Science* **299** 862-864 (2003)

[25] Brunner N, Huber M, Linded N, Popescu S, Silva R, Scrzypczyk P. Entanglement enhances cooling in microscopic quantum refrigerators. *Phys. Rev.'E* **89** 032115 (2014)

[26] Hardal A C and Mustecaplioglu O. Superradiant Quantum Heat Engine. arXiv:1503.03797 (2015)

[27] Binder F C, Vinjanampathy S, Modi K and Goold J. Quantacell: powerful charging of quantum batteries. *New J. Phys.* **17** 075015 (2015)

[28] Roßnagel J, Abah O, Schmidt-Kaler F, Singer K and Lutz E. A nano heat engine beyond the Carnot limit. *Phys. Rev. Lett.* **112** 030602 (2014)

[29] Rober Alicki, David Gelbwaser-Klimovsky Nonequilibrium quantum heat machines. *New J. Phys.* **17** 115012 (2015)

[30] Ciccarello F. Collision models in quantum optics. *Quantum Meas. Quantum Metrol.* **4** 53 (2017)

[31] Ciccarello F and Giovannetti V. A quantum non-Markovian collision model: incoherent swap case. *Phys.*

Scr. **T153** 014010 (2013)

[32] McCloskey R and Paternostro M. Non-Markovianity and System-Environment Correlations in a microscopic collision model. *Phys. Rev. A* **89** 052120 (2014)

[33] Lorenzo S, McCloskey R, Ciccarello F, Paternostro M and Palma G M. Landauer's Principle in Multipartite Open Quantum System Dynamics. *Phys. Rev. Lett.* **115** 120403 (2015)

[34] Kretschmer S, Luoma K and Strunz W T. Collision model for non-Markovian quantum dynamics. *Phys. Rev. A* **94** 012106 (2016)

[35] Pezzutto M, Paternostro M and Omar Y. Implications of non-Markovian dynamics for the Landauer bound. *New J. Phys.* **18** 123018 (2016)

[36] Cakmak B, Pezzutto M, Paternostro M and Mustecaplioglu E. Non-Markovianity, coherence, and system-environment correlations in a long-range collision model. *Phys. Rev. A* **96** 022109 (2017)

[37] Campbell S, Ciccarello F, Palma G M and Vacchini B. System-environment correlations and Markovian embedding of quantum non-Markovian dynamics. arXiv:1805.09626 (2018)

[38] Lorenzo S, Ciccarello F, Palma G M and Vacchini B. Quantum non-Markovian piecewise dynamics from collision models. arXiv:1706.09025 (2017)

[39] Deffner S and Lutz E. Nonequilibrium work distribution of a quantum harmonic oscillator. *Phys. Rev.E* **77** 021128 (2008)

[40] Husimi K. The forced harmonic oscillator. *Progress of Theoretical Physics* **9** 4 (1953)

[41] Here, and only within this section, we use the letter n as superscript to label the particle with which the engine interacts, and *not* the excitation number of the harmonic oscillator, as in the rest of the article.

[42] Scarani V, Ziman M, Stelmachovic P, Gisin N and Buzek V. Thermalizing Quantum Machines: Dissipation and Entanglement. *Phys. Rev. Lett.* **88** 097905 (2002)

[43] Rivas, Huelga S F and Plenio M B. Entanglement and Non-Markovianity of Quantum Evolutions. *Phys. Rev. Lett.* **105** 050403 (2010)

[44] Breuer H-P, Laine E-M and Piilo J. Measure for the Degree of Non-Markovian Behavior of Quantum Processes in Open Systems. *Phys. Rev. Lett.* **103** 210401 (2009)

[45] Laine E-M, Piilo J and Breuer H-P. Measure for the non-Markovianity of quantum processes. *Phys. Rev. A* **81** 062115 (2010)

[46] Nielsen M A and Chuang I L. *Quantum Computation and Quantum Information - 10th Anniversary Edition* (Cambridge: Cambridge University Press) p. 403 (2010)

[47] Wissmann S, Karlsson A, Laine E-M and Breuer H-P. Optimal state pairs for non-Markovian quantum dynamics. *Phys. Rev.* A **86** 062108 (2012)